Computer Simulation of Corrosion Fatigue Process Considering Stress Relaxation Due to Initiation and Propagation of Multiple Cracks*

Sotomi ISHIHARA**, Kazuaki SHIOZAWA**,
Kazyu MIYAO** and Hiroshi MIWA**

In order to investigate stress relaxation behavior at the specimen surface during the corrosion fatigue process caused by the initiation and propagation of many cracks, rotating bending fatigue tests were carried out in sodium chloride aqueous solution using specimens of 6 and 12 mm diameters. Stress amplitude decreases of about 25 ~50% were observed during the corrosion fatigue process performed at low stress amplitude. This stress relaxation behavior is well evaluated by calculating the compliance increase of the specimen. Computer simulations of the corrosion fatigue process of the unnotched specimens were conducted. The results showed good agreement with the experimental results. In the simulations, probabilistic crack initiation behavior during the corrosion fatigue process, the stress relaxation effect at the cracked parts and crack coalescences among many distributed cracks are taken into consideration.

Key Words: Corrosion Fatigue, Computer Simulation, Stress Relaxation, Size Effect, Distributed Surface Cracks, Crack Coalescence

1. Introduction

It is well known that many small surface cracks initiate on the smooth specimen surface during corrosion fatigue. It is considered[1),(2)] that the interferences and the coalescences among these cracks control the corrosion fatigue lives. In the previous paper[3)], we investigated the relationships between corrosion fatigue lives and the characteristics of the distributed cracks, such as the number of cracks and the sum total of crack lengths, using round specimens with different diameters (6 mm and 12 mm). It was clarified that corrosion fatigue lives for the specimens of 12 mm diameter increase with increasing number of cracks initiated during the corrosion fatigue process; on the other hand, the opposite tendency was observed for the specimens of 6 mm diameter. For this reason, it was considered that the crack coalescence among the distributed surface cracks was the main factor influencing corrosion fatigue lives for the specimens of 6 mm diameter, while the stress relaxation effect at the cracked part was an important factor determining corrosion fatigue lives for the specimens of 12 mm diameter.

In the present paper, the stress relaxation effect stated above was investigated experimentally and theoretically. Further, we performed a computer simulation of the corrosion fatigue process where the stress relaxation effect was taken into consideration, in addition to the crack coalescence behavior, and confirmed the validity of the simulation from the comparison of the results of the simulation with experimental results.

2. Specimen and Experimental Procedures

The material tested was J.I.S. carbon steel S45C. As-received materials were annealed at 1 173K in vacuum for 1 hour and then electropolished preceding the fatigue tests. Its chemical composition and mechanical properties are listed in Table 1 and Table 2 respectively. The shapes and dimensions of the specimens are shown in Fig. 1. Corrosion fatigue tests were performed in the low stress amplitude region (98 MPa) where the effect of the distributed surface

* Received 29th July, 1991. Paper No. 90-0419B
** Faculty of Engineering, Toyama University, 3190 Gofuku, Toyama 930, Japan

cracks on the fatigue lives is assumed to be marked, using both the specimens of 6 mm and 12 mm diameter. An Ono-type rotating bending fatigue machine was used, and its frequency was 60 Hz. As a corrosive environment, sodium chloride aqueous solution kept at 298 K was used in the present tests.

The variations of the strains at the cracked parts of the specimen were investigated successively during the corrosion fatigue process, using straingauges whose gauge length was 0.2 mm. In order to obtain the average variations of the strains due to the crack initiations and propagations, we measured them at several points in the specimen. The cracks initiated at that time in those places were also measured using the surface replica.

3. Experimental Results

3.1 Variations of the strain at the cracked parts in the specimen with an increase in the applied bending moment

In order to investigate the variations of each specimen's stiffness due to crack initiations, a corrosion fatigue test was performed at the stress amplitude of 98 MPa and stopped before final failure of the specimen. Figure 2 shows examples of the relationships between the maximum strains in the specimen and the applied bending moment. The solid lines in this figure correspond to the relationships after crack initiation measured at several places in the specimen, and the broken line represents that before crack initiation. As seen from this figure, the surface strains at the cracked parts are smaller than that before crack initiation. Supposing that Young's modulus of the material is not changed by the crack initiation, we can consider the decrease in the strain as the decrease in the stress. Therefore, we realize that the applied stresses at each point of the specimen surface during the corrosion fatigue process are decreased by the crack initiation and the crack growth.

Table 1 Chemical compositions of the material
(Wt %)

C	Si	Mn	P
0.46	0.23	0.81	0.022

Table 2 Mechanical properties of the specimen

Yield Point	Tensile Strength	Elongation
317MPa	624MPa	48.7%

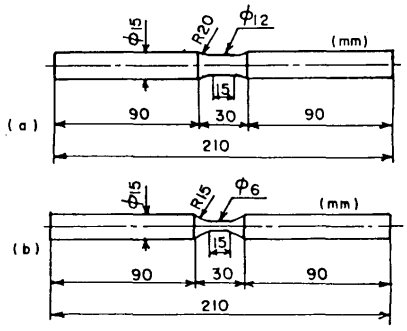

Fig. 1 Shape and dimensions of the specimen

3.2 The effect of the distributed surface cracks on the stress relaxation at the specimen surface

Figure 3 shows the relationship between $\varepsilon^*/\varepsilon$ and sum total of crack lengths $(1/A)\sum 2l_i$ obtained in the corrosion fatigue test of 98 MPa, where ε^* is a strain at the specimen surface after crack initiation and ε is that before the fatigue test. A is an area where crack lengths are investigated. We can consider the decrease

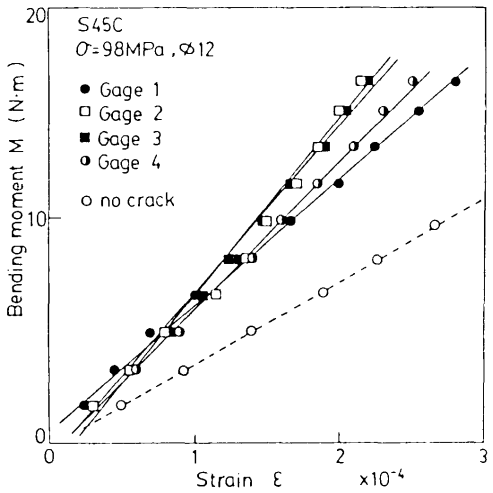

Fig. 2 Relationships between bending moment and strain at the cracked parts in the specimen

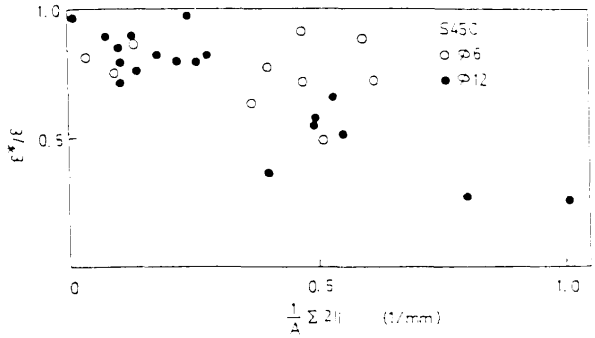

Fig. 3 Variations of the normalized strain with sum total of crack lengths for both 6 and 12 specimens

in the strain to be equivalent to that in the stress.

As seen from this figure, $\varepsilon^*/\varepsilon$ decreases with increase in the $(1/A)\sum 2l_i$ for both specimens of 6mm and 12 mm diameters. Figure 4 shows the variations of $\varepsilon^*/\varepsilon$ with the number of cycles after crack initiation $(N-N_i)$. We can see that the values $\varepsilon^*/\varepsilon$ for the specimen of 12 mm diameter decrease markedly compared with those for the specimen of 6 mm diameter.

4. Estimation Method of the Stress Relaxation Effect at the Cracked Parts

4.1 Aboudi's method[4]

Aboudi[4] treated the problem shown in Fig. 5(b) in which the fixed displacement in the X_1 direction is given to an infinite plate with equally spaced cracks. He calculated the compliance change of the plate by introducing the unitcell, and dividing this into two parts, as shown in Fig. 5(a), that is, the region ($a=1$) where one crack exists and the region ($a=2$) where no cracks exist. A brief outline of his calculation is shown as follows.

Averaging the equilibrium equations for both regions in the X_3 direction, we can obtain the following equation:

$$\partial_1 S_{ij}^{(k)(a)}+(d_a/2)^k[\sigma_{3j}^{(a)}(d_a/2)$$

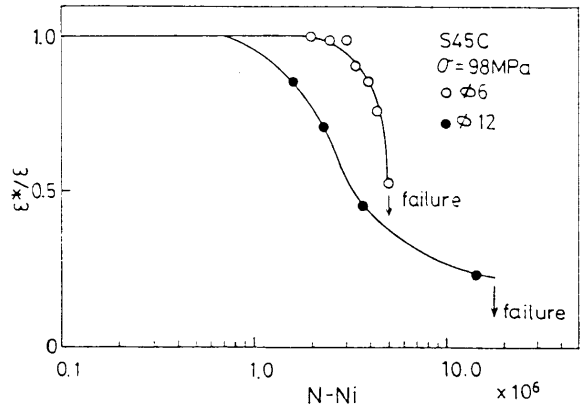

Fig. 4 Variations of the normalized strain during stress cycling

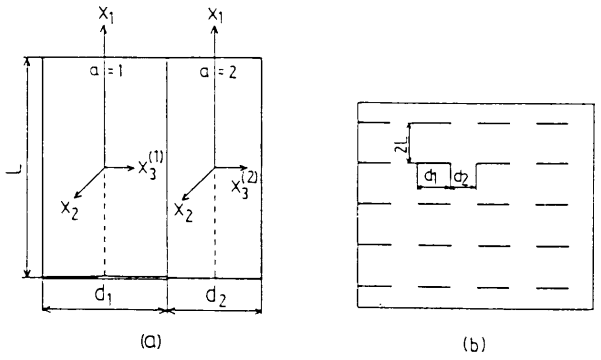

Fig. 5 Aboudi's model for the calculation of the stiffness reduction of the plate due to cracks

$$+(-1)^{k+1}\sigma_{3j}^{(a)}(-d_a/2)]/d_a-kS_{3j}^{(k-1)(a)}=0, \quad (1)$$

where, $\sigma_{ij}^{(a)}$ denotes the stresses in these regions and $S_{ij}^{(k)(a)}$ denotes the average stresses defined as follows.

$$S_{ij}^{(k)(a)}=(1/d_a)\int_{-da/2}^{da/2}(X_3^{(a)})^k\sigma_{ij}^{(a)}dx_3^{(a)} \quad (k=0,1,2) \quad (2)$$

Using the boundary conditions for the stresses, the strain-deformation relation and the stress-strain relation, we can resolve Eq.(1). The effective elastic modulus of the unit cell in the X_1 direction can be obtained. Aboudi arranged the calculated results in a manner of using both the parameters of $d_1/(d_1+d_2)$ and $d_1/2L$.

In the present study, the dimension d_1 was determined by dividing the sum total of crack lengths in the observed area with the total number of cracks. Further,the dimensions of d_2 and $2L$ were determined in such a way that n_t cracks with the length of d_1 were arranged regularly, as shown in Fig. 5(b). As it was impossible to resolve Eq.(1) analytically, we resolved it numerically using the finite difference method.

In the rotating bending tests, bending moment applied to the specimen is constant during the fatigue test. However, at the cracked parts in the specimen, the local stresses are relieved and redistributed complexly by the compliance change due to the crack initiations. Thus, in the present study, we obtained the stresses at the cracked parts by assuming that the applied displacements near the specimen surface are constant before and after crack initiation.

4.2 Estimation of the amount of the stress relaxation due to an increase in the compliance at the cracked parts

In addition to Aboudi's method[4], we evaluated the amount of stress relaxation at the cracked parts using the compliance method[5]. Let us consider a round bar specimen whose length and diameter are L_c and d, respectively. Bending moment is applied to this bar, and it contains n cracks at time J. The amount of the compliance increase due to these crack initiations is given by the following equation[5].

$$\Delta\lambda_j=\sum_{i=1}^{n}\int_0^{Ai}\frac{2}{E}\left(\frac{K_B}{M}\right)dA_i \quad (3)$$

The compliance for the specimen with no cracks is given by

$$\lambda_0=\frac{L_c}{EI} \quad (4)$$

where A_i denotes the each crack area and E and I are Young's modulus and moment of inertia of area, respectively. K_B is a correction factor for the cracked round bar specimen under bending.

The compliance at time J is calculated by the next equation,

$$\lambda_j=\lambda_0+\Delta\lambda_j, \quad (5)$$

where $\triangle\lambda_j$ is the compliance increase due to crack initiation.

Using the same assumptions as in Aboudi's method[4], that is, (i) the applied displacement is constant at the specimen surface, and (ii) Young's modulus is constant before and after crack initiation, we can estimate the variations of stresses at the cracked parts. There is the following relationship between the stress at time J and the one at time J-1:

$$\sigma_j=\frac{\lambda_0+\lambda_{j-1}}{\lambda_0+\lambda_j}\sigma_{j-1} \quad . \qquad (6)$$

Figures 6 and 7 show the estimated results using Aboudi's method and the compliance method, respectively. As seen from Fig. 6, the calculated results coincide well with experimental results in the region $(1/A)\sum 2l_i < 0.5$. However, in the region $(1/A)\sum 2l_i > 0.5$, the estimated results for the 12 specimen are larger than the experimental results. In the region $(1/A)\sum 2l_i > 0.5$, there are initiated a few long cracks which cause a large amount of stiffness decrease in the specimen; thus, the situation is not appropriate for the model shown in Fig. 5(b). This is why the experimental and theoretical results do not coincide with each other in the region $(1/A)\sum 2l_i > 0.5$. In Fig. 7, on the other hand, the estimated results using the compliance method show good agreement with the experimental results because the method takes the real crack lengths on the specimen surface into consideration. As a result, in the computer simulation of the corrosion fatigue process stated below, we shall use the compliance method for the calculation of the stress variation at the cracked parts.

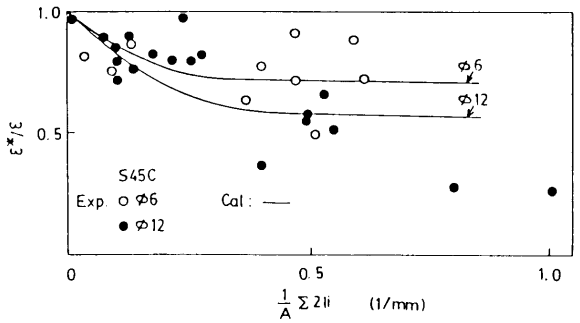

Fig. 6 Comparison with the calculated results obtained from the Aboudi's model and the experimental results

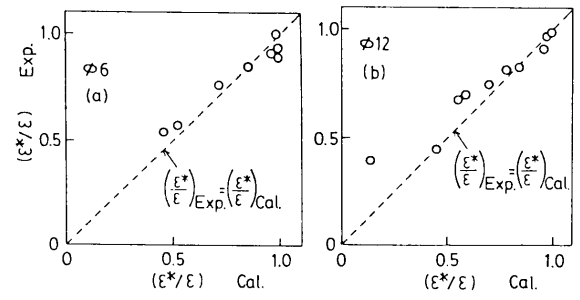

Fig. 7 Comparison with the calculated results for the normalized strain obtained from the compliance method and the experimental results

5. Computer Simulation of the Corrosion Fatigue Process Considering the Stress Relaxation at the Cracked Parts

5.1 Flow chart of the simulation

We performed a computer simulation of the corrosion fatigue process for unnotched specimens. In the previously reported simulation program, the probabilistic crack initiation behavior and crack coalescence behavior were considered. In the present simulation, the subroutine for the calculation of the stress relaxation effect at the cracked parts is newly added to the previous program.

The flow chart of the program is shown in Fig. 8. The frame drawn by the thick solid line in this figure shows the subroutine for evaluating the stress relaxation effect.

5.2 Input data

The input data for the simulation are listed as follows:

(a) Maximum crack density: Three-parameters of Weibull distribution reported in the previous study[3] were employed.

(b) The rate of crack initiation: Three-parameters of Weibull distribution reported in the previous

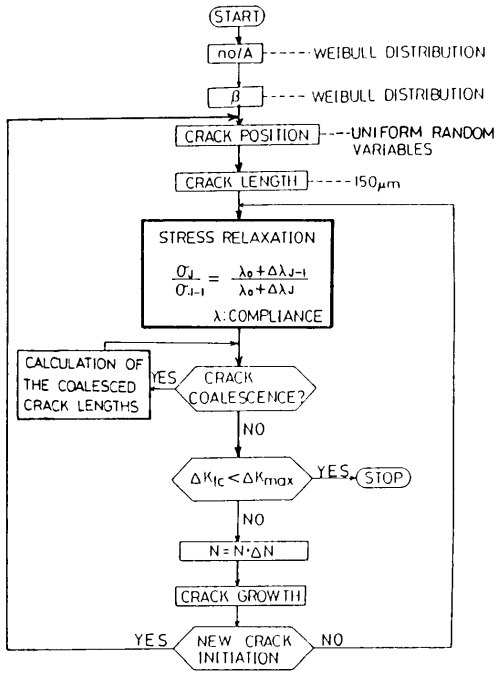

Fig. 8 The flow chart for the computer simulation of the corrosion fatigue process

study[3] were employed.

(c) Crack location: Uniform random distribution was used.

(d) Initial crack length: It was designated as 150 μm.

(e) Crack growth: The crack growth behavior was prescribed by Paris's equation,

$$dl/dN = C\{\sigma(\pi l)^{1/2}\}^m$$

where C and m were experimentally determined as $C = 1.654 \times 10^{-11}$ and $m = 2.41$.

(f) The criterion for the final failure of the specimens: The following criterion was adopted for the final failure of the specimen. When the maximum stress intensity factor among the many surface cracks reaches the fatigue fracture toughness in the corrosion fatigue, which is determined as 9 $MPam^{1/2}$, final failure of the specimen occurs.

(g) Threshold condition: $\Delta K_{th} = 0.0$ $MPam^{1/2}$ was adopted.

5.3 Comparison between the experimental results and the results from the computer simulation

Figure 9 shows an example of the crack initiation and growth obtained from the computer simulation of the corrosion fatigue process for both $\phi 6$ and $\phi 12$ specimens. Figure 10 shows the main crack growth behavior obteined from the simulation which causes the final failure of the specimen. In these figures, experimental results are also plotted. As seen from Fig. 10, both the acceleration of the crack growth rate through crack coalescences and the retardation of the crack growth rate due to the stress relaxation at the cracked parts are simulated well.

Figure 11 shows the variation of the distributions of crack lengths during corrosion fatigue process which are obtained from the computer simulation. The experimentally obtained results are also shown by the solid and broken lines in this figure. Good agreement between the two is observed. The parts bent downward in the region of long crack length in the experimental results correspond to the occurrence of long cracks due to crack coalescences.

Many trials of the simulations were performed and the relationship between the crack growth period

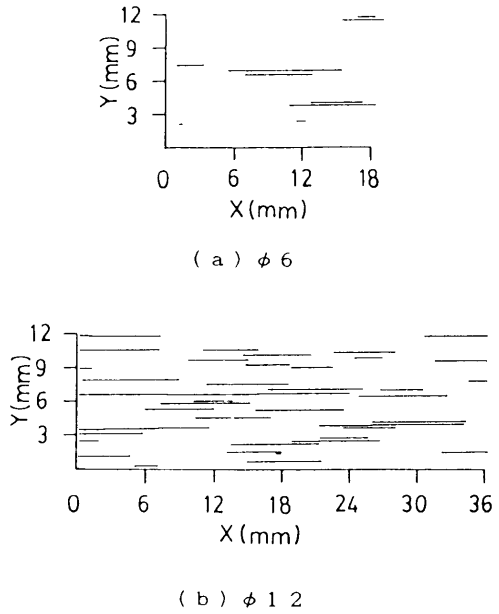

Fig. 9 An example of the spatial distribution of cracks in the computer simulation

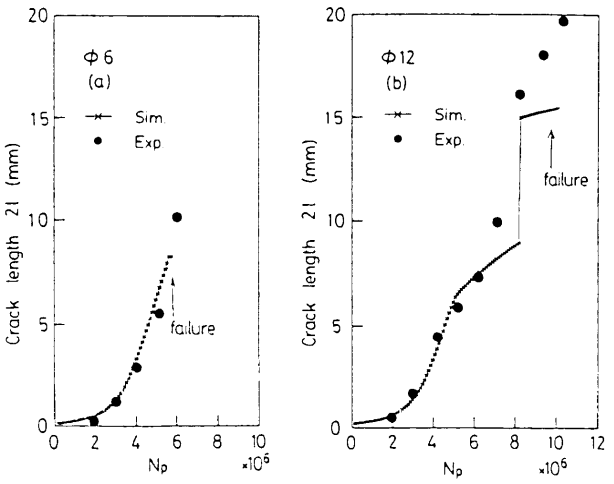

Fig. 10 The main crack growth behavior which causes final failure of the specimen

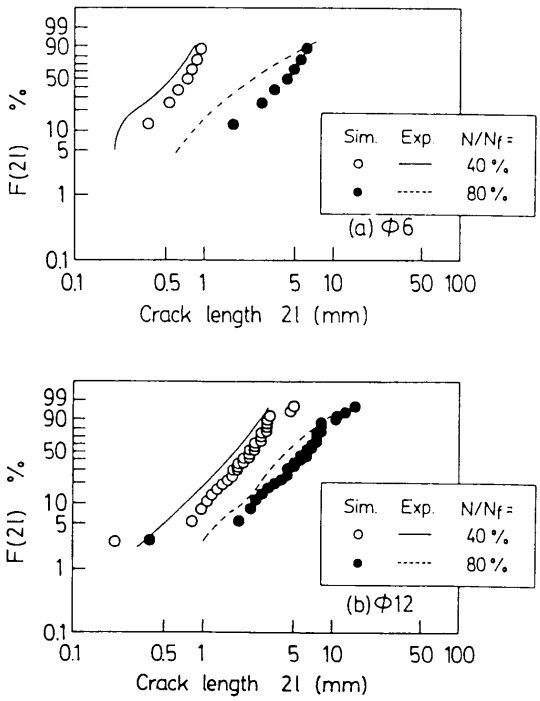

Fig. 11 Variations of the distributions of crack lengths with stress cycling

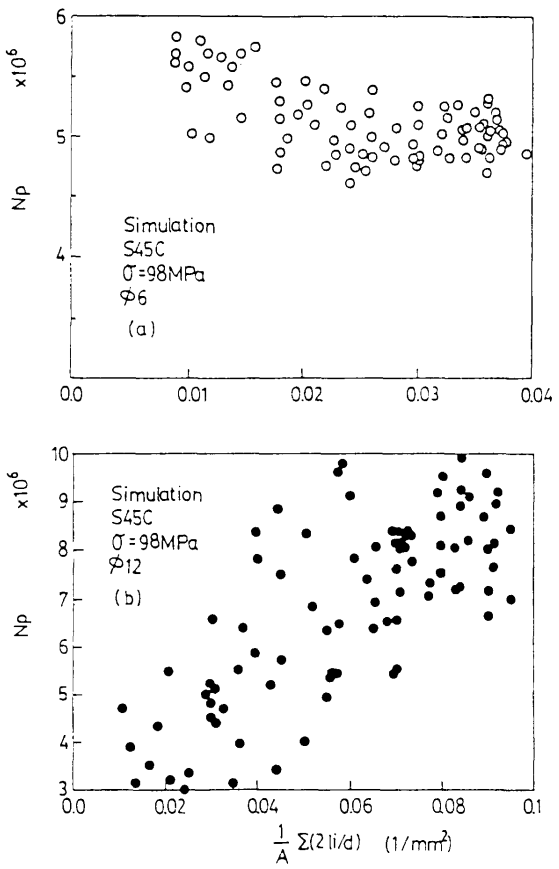

Fig. 12 Relationships between the crack growth periods and sum total of crack lengths

N_p and the sum total of crack lengths per area $(1/A)\Sigma(2l_i/d)$ was investigated. Figure 12 shows the results. In the $\phi 6$ specimens, N_p decreases with an increase in $(1/A)\Sigma(2l_i/d)$. In the $\phi 12$ specimens, on the other hand, the reverse tendency is observed. These results obtained from the computer simulation show the same tendency as the experimentally obtained one reported in the previous paper[3].

6. Conclusions

Computer simulations of the corrosion fatigue process were performed. The results obtained are summarized as follows:

(1) The stress relaxation behavior at the cracked parts in the specimen during the corrosion fatigue process was investigated in detail experimentally and theoretically. It was clarified that the effects were evaluated well from the calculation of the amount of increase in the compliance at the cracked parts.

(2) The amount of stress relaxation at the cracked parts during the corrosion fatigue process was investigated experimentally. The effects begin to be observed from the time $N/N_f=0.3$. The maximum stress decreases at the final failure of the specimen were 25% and 50% for $\phi 6$ and $\phi 12$ mm specimens, respectively.

(3) Computer simulations of the corrosion fatigue process in which the probabilistic crack initiations, crack coalescences and the stress relaxation effect were taken into consideration were performed. The results showed good agreement with the experimental results.

References

(1) Kitagawa, H., Fujita, T. and Miyazawa, K., Small Randomly Distributed Cracks in Corrosion Fatigue, ASTM Spec. Tech., 642(1978), p. 98.

(2) Ishihara, S., Miyao, K. and Maekawa, I., Effects of the Distribution of Multiple Surface Cracks on Fatigue Life of a Shot-Peened Specimen, Trans. Jpn. Soc. Mech. Eng., (in Japanese), Vol. 54, No.507,A (1988),p. 1967.

(3) Ishihara, S., Miyao, K. and Miwa, H., Effects of Distributed Surface Cracks on Corrosion Fatigue Lives of Specimens with Different Diameters, Trans. Jpn. Soc. Mech. Eng., (in Japanese), Vol. 55, No. 514, A(1989), p. 1275.

(4) Aboudi, J., Stiffness Reduction of Cracked Solids, Eng. Fract. Mech., Vol. 26, No. 5(1987), p. 637.

(5) Okamura, H., An Introduction to Linear Fracture Mechanics, (in Japanese), (1976), p. 101, Baifukan.